Proceedings of ISFOG 2025
5TH INTERNATIONAL SYMPOSIUM ON
FRONTIERS IN OFFSHORE GEOTECHNICS
Nantes, France | June 9-13 2025

ISBN 978-2-85782-758-0

PROSE+ project: offshore seismic measurements on the seabed to test the ability to assess the spatial variation of the small-strain shear modulus in the subsurface environment

Tartoussi, N [1]., Leparoux D. [1], Michel L.[2], Evain M.[3], Lehujeur M.[1], Allemand T.[2], Pelleau P.[3], Josse F.[2], Rousset J.M.[4], Belov S.[3], Schnurle Ph.[3], Sourice A.[2], Baltzer A.[5]

[1] *GERS-GeoEND / Université Gustave Eiffel - OSUNA , Bouguenais, France*
[2] *Sercel company, carquefou, france*
[3] *Geo-Ocean / Ifremer, Brest , France*
[4] *Nantes Université - Ecole Centrale de Nantes , Nantes, France*
[5] *LETG / Nantes Université – OSUNA , Nantes, France*

donatienne.leparoux@univ-eiffel.fr (correspnding author)

ABSTRACT: The increase in the number of offshore wind farm siting projects, combined with the multiplicity of developments in anchoring techniques, means that foundations and anchors need to be optimized for the conditions of the offshore subsurface, requiring precise knowledge of the mechanical characteristics of the medium. According to the recommendations of the CFMS (French committee of Soils Mechanics), detailed geophysical reconnaissance is then necessary during the project phase (design and execution) to obtain the most accurate information possible at the locations of the structures. In this context, the PROSE+ project aims to increase knowledge and provide new methodological and technical elements, based on surface seismic and geoelectrical techniques. This will make possible to approach heterogeneous environments in a quantitative and non-destructive way, thereby reducing the number of costly and invasive geotechnical surveys. To this end, we developed numerically a 2D seismic inversion technique using Surface Seismic Waves based on Particle Swarm optimization methods. In order to validate it on experimental data, we carried out measurements off Concarneau using 70 4-components sensors (GPR - Sercel nodes) placed on the seabed, in an unprecedented manner. 241 seismic shots were fired over this sensor's network using an air gun at variable water depth. Finally, the sensors were left recording on the seafloor for 28 days. The recorded seismic data allow to test the capacity of both active and passive seismic imaging process to assess the shear modulus in a 2D medium under seabed.

Keywords: seismic surface waves; seabed sensors; shear waves velocity; shear modulus passive recordings

1 INTRODUCTION

For the development of offshore wind turbines in a variety of geologically complex contexts, detailed knowledge of the mechanical characteristics of the marine subsoil and their spatial variations is required both at depth over the first 30 meters and laterally around each anchoring or foundation position. However, geotechnical surveys are expensive, destructive and provide only localized information. For this reason, the CFMS (Comité Français de Mécanique des Sols) (Berthelot et al., 2019) recommends the use of geophysical information, including the seismic surface waves approach. Indeed, in the terrestrial domain, a number of studies show the possible correlation between geotechnical parameters and seismic parameters, notably through the small-strain shear modulus Gmax, accessible from S waves velocity parameter assessed by inversion of the seismic surface waves dispersion (e.g. Wang et al, 2024).

A number of previous geophysical studies have focused on the inversion of seismic Vs shear wave velocities in the seabed from Scholte waves, which are surface waves developed at the seabed interface (e.g. Klein et al., 2005 ; Strobbia et al., 2006 ; Vanneste et al., 2011). These works propose instrumentation using hydrophones or OBCs (accelerometers) without comparing the benefits of these two types of sensor with each other. In these various works, the source used is an air-gun close to the surface or between two waters, or a vibrating source on the seabed. The latter seems well-suited to generating Sholte waves, but it is heavy to install and difficult to move. Finally, these studiers make the usual assumption of 1D media (or series of 1D media) for the estimation of the Vs velocity model by the MASW method.

In this context, the PROSE+ project aims to develop a 2D methodology for the reconstruction of subsurface mechanical characteristics through Vs velocity and Gmax modulus (Pageot, D. et al. (2018)). The first phase of the project aims to test adapted and optimized seabed instrumentation for generating and recording Sholte waves by comparing the recordings of different sensors and the effects of different types of air-gun positions, which remains a light, easy-to-move source.

To this end, we carried out a campaign of active and passive seismic measurements off Concarneau in France (South Brittany region), using seafloor sensors (4 components) at a depth of 28 m, left unattended for 28 days, and several air-gun source positions.

The different positions and depths of the air-gun shots, as well as the so-called "passive" recordings, and the comparison of recordings on each of the components make possible to compare the effectiveness of the configurations for recording Scholte waves.

2 MEASUREMENT CONFIGURATION

2.1 Receivers setup

The measurement campaign detailed in this article was carried out in the South Brittany region, off the French coast, southwest of Concarneau. 70 4-component sensors (GPR Sercel), comprising 3 oriented accelerometers and a hydrophone, were deployed at a depth of 28 m using a winch workboat winch (Figure 1). Verification of the alignment and orientation of each sensor was then carried out by ifremer divers. As a result, a configuration of 5 parallel lines was deployed according to the geometry shown in Figure 2. The central line of 50 sensors spaced 2 m apart provided a measurement profile 98 m long, while the lateral lines on either side consisted of 7 and 3 sensors spaced 10 m and 20 m apart respectively. 240 airgun shots were fired on either side of each line at 3 different depths: 5 m, 13 m and 22 m. Finally, a network of seismic shots was fired in a circle around the entire system. The positions were then estimated by inversion of the time of the first arrival: the direct acoustic wave from the source. Figure 2 shows all the positions found by inversion.

Figure 1 – 4-component seismic sensors (Sercel GPR nodes) placed on the seabed (28 m depth)

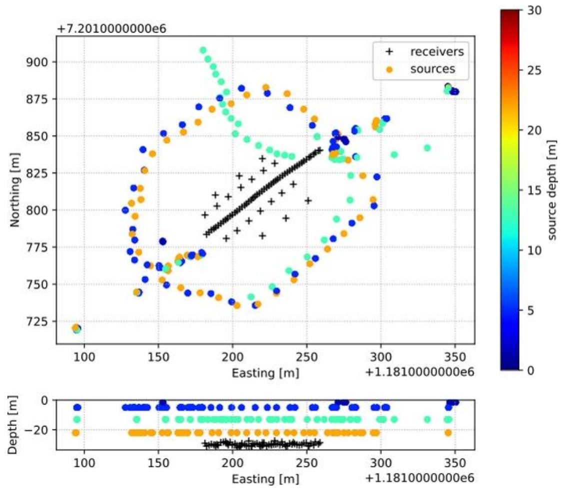

Figure 2 –positions of seabed sensors for the seismic campaign off Concarneau. Black crosses: source positions, circles: receiver positions. Each color corresponds to a specific depth indicated on the profile below the map.

3 ANALYSIS OF DATA ACQUIRED BY ACTIVE SOURCES

3.1 Hydrophone and vertical accelerometers

First of all, before any analysis, the measurements must be corrected for clock drift. Figure 3 and Figure 4 show the raw data recorded by the vertical accelerometers along the central line of the receivers before and after correction for clock drift respectively. The consistency of seismic arrivals after clock correction is clearly visible.

Figure 5 shows the equivalent shot to the previous one, but recorded with the hydrophones. The clock-corrected arrivals are not only coherent, but also show a very regular wavelet shape, whereas the accelerometer recordings show variations in the signal shapes along the measurement line and the presence of ringing effects around sensor N°15. However, the quality of the information conveyed by the signals must be viewed through the dispersion diagrams, calculated by p-omega transformations (Park et al., 1998). In this dispersion diagrams, the maxima lines (in red color in Figures 6, 7, 8, 9, 10, 11) indicate the phase velocity curves of the recorded signals, as a function of frequency. For further works of imaging process, these diagrams will be the input parameters for the inversion approach in order to estimate the velocity profile Vs of the medium.

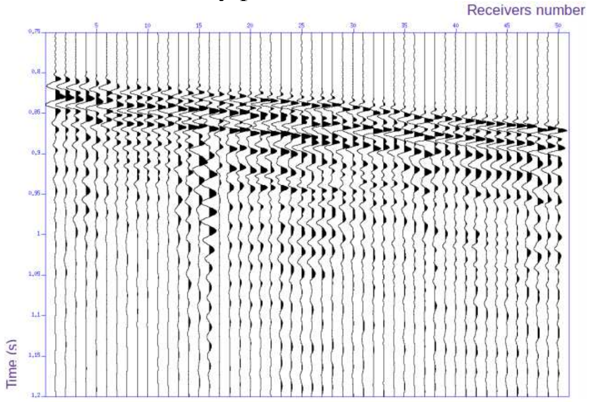

Figure 3 –example of a seismic shot recorded on the central receiver line, from the vertical component of the accelerometers

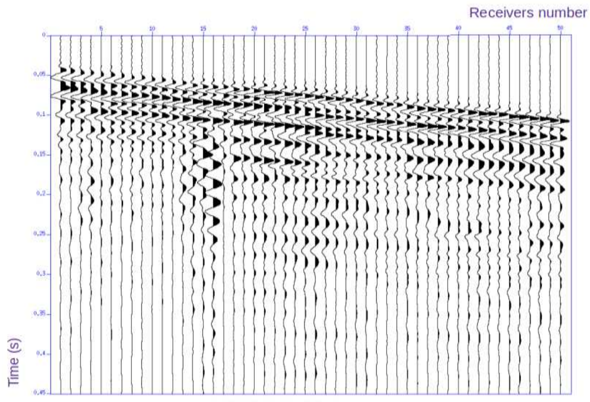

Figure 4 –seismic shot shown in figure 3 after clock drift correction.

Figure 6 shows the dispersion diagrams of the data shown in Figures 4 and 5 from accelerometer and hydrophone recordings respectively (Park et al., 1998). The latter diagram (Figure 6 – right part) shows a very regular maximum (in red), identifying a phase velocity that is easy to determine up to frequencies of 200 Hz. The diagram from the vertical component of the accelerometers, on the other hand, is more complex. It features two modes in the low-frequency range and a distinct high-frequency mode, with phase velocities around 2500 m/s for the latter. These are acoustic waves propagated in the water column. The modes identified at low frequencies (below 30Hz) are characteristic of Scholte waves, i.e. surface waves propagating at the soil/water interface, depending o the soil characteristics. This is the part of the diagram which is needed to recover the S waves velocities of the undergorund medium.

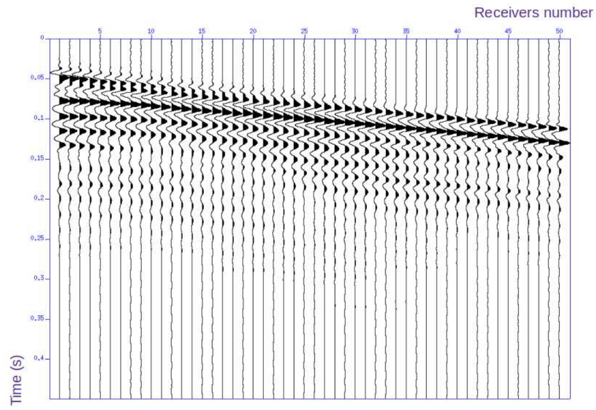

Figure 5 – example of a seismic shot (after correction for clock drift) recorded by the hydrophones of the central line of receivers. Source identical to that used for the recording shown in figures 3 and 4.

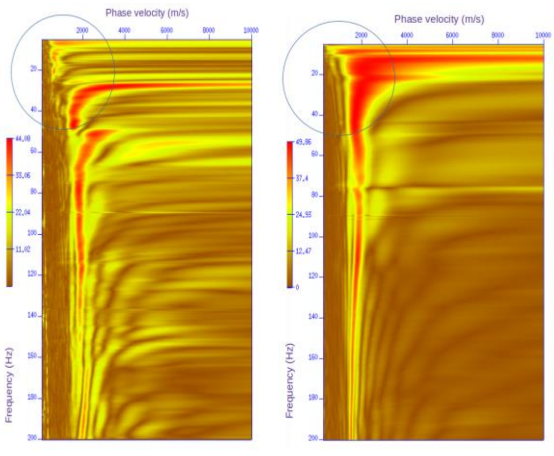

Figure 6 – example of dispersion diagrams calculated for one shot recorded by central line receivers - left: accelerometers vertical components - right: hydrophones.

These dispersion diagrams shows how the use of seismic bottom sensors recording the particular acceleration is more appropriate for recording the Sholte wave than hydrophones. Note that dispersion diagrams calculated with the in-line coponents are intermediar quality (Figure 7).

Finally, Figure 8 shows a zoom of the dispersion diagrams from the data shown in right side of Figure 6 before and after clock correction. It can be seen here that clock correction enables a more accurate estimation of phase velocities, particularly between 15 and 20 Hz, even if the difference in results remains weak.

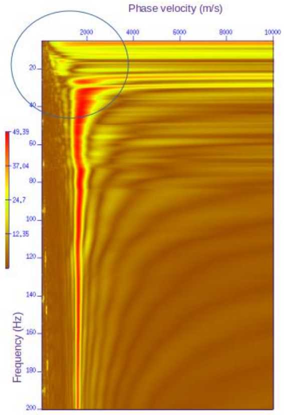

Figure 7 – dispersion diagram calculated for the same shot as figure 6 for the accelerometers in-line components.

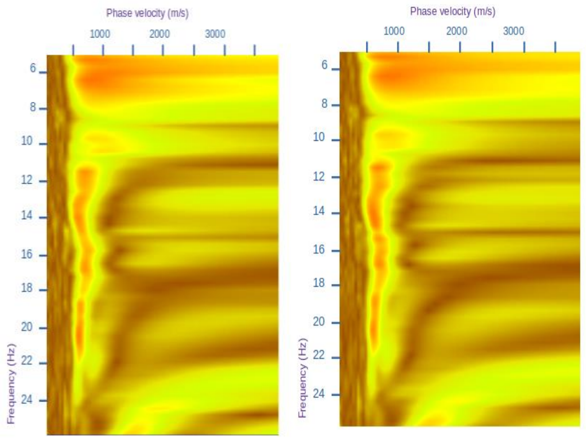

Figure 8 – Zoom of dispersion diagrams calculated for shots recorded by central line accelerometers (vertical component) – left : before clockdrift correction – right : after clockdrift correction.

3.2 Source position

The multiple source positions tested during the measurements make it possible to compare the effects of the depth of the airgun source and the minimum distance between source and receiver on the surface wave content in the data.

Figure 9 shows a zoom on the first 50 Hz of the dispersion diagrams calculated from the signals recorded by the vertical component of the accelerometers on the central line for a minimum source-receiver distance of 5 m and different air-gun depths: 5m, 13 m and 22 m respectively . We note that when the source is close to the seabed, the dispersion diagrams contains information around 10 Hz that is not visible for shallower source positions (lower frequency part in the blue circle on Figure 9). However, these diagrams remain less clear for the "Scholte wave" part than those shown in the previous section. The minimum distance of 5 m is probably ill-suited to the development of surface waves at frequencies of 10 to 30 Hz, corresponding to long wavelengths around 15 à 85 m. To confirm this hypothesis, Figure 10 shows a zoom on the low-frequency part of the dispersion diagrams calculated for recordings from air-gun shots at 30 m offset for the three depths tested. A higher coherent energy is observed in the low frequency range (below 12 Hz) for the deepest air-gun position (right-hand diagram in Figure 10). Finally, Figure 11 shows diagrams calculated from recordings for the airgun source positioned at a depth of 22 m, but for 3 specifical minimum offsets equal to 12 m , 20 m and 30 m respectively. These results clearly show the higher contribution of information in surface waves for a minimum offset of 30 m.

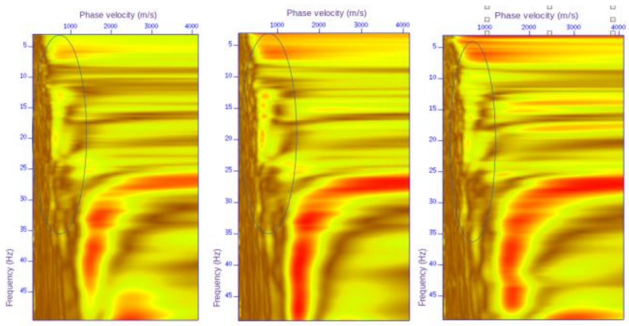

Figure 9 – Dispersion diagrams calculated for shots recorded by central line accelerometers (vertical component) with a minimum offset equal to 5 m and for different source depth – left : 5 m ; centre : 13 m ; right : 22 m.

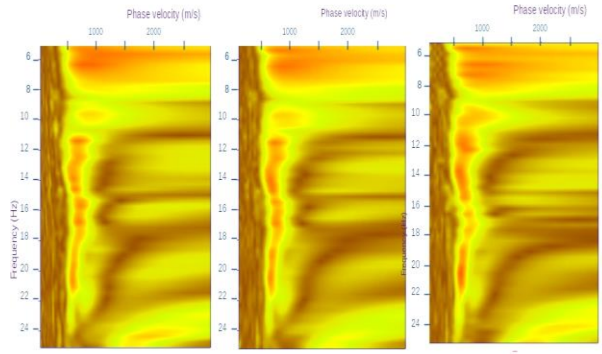

Figure 10 – Zoom on dispersion diagrams calculated for shots recorded by central line accelerometers (vertical component) with a minimum offset equal to 30 m and for different source depth – left : 5 m ; centre : 13 m ; right : 22 m.

The wavelengths recorded on this dispersion diagrams are between 15 m and 85 m. They will be used to estimate the velocity of shear waves, linked to the small-strain shear modulus over a depth around 5 to 30 m in the subsoil.

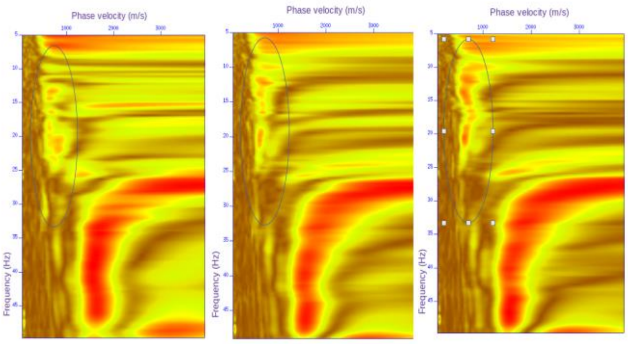

Figure 11 – Dispersion diagrams calculated for shots recorded by central line accelerometers (vertical component) for a source depth equal to 22m and different minimum offset – left : 12 m ; centre : 20 m ; right : 30 m

4 ANALYSIS OF DATA ACQUIRED IN PASSIVE MODE

The air-gun campaign was supplemented by so-called passive recordings (Draganov et al., 2015), with the 70 sensors left in place for 26 days. During the 26 days of passive recording that followed the active phase, the four sensors equipping each GPR node performed optimally. The quality of these records was assessed by Probabilistic Power Spectral Density (PPSD) analysis. These histograms reveal that in the low frequency band, below 1 Hz, seismic records are dominated by microseismic noise. The latter is an ubiquitous signal that travel great distances within the Earth. It can be generated at distant or local seafloor by pressure waves traveling vertically from swells on sea surface. In the high frequency band, a broad amplitude peak is visible centered at 10 Hz that probably results from various sources of vibration that need to be understood. Our first approach has been to focus on these high frequency range that is common with the active experiment. Cross-correlating passive records between pairs of nodes enable to enhance low amplitude but coherent seismic signal recorded at two distant locations. We use the 26 days of records from vertical sensors and cross-correlated all possible pairs of nodes deployed along the central line of the experiment (Figure 12). This processing is widely employed on land seismic experiment to reveal surface and/or body waves propagating beneath a sensor network and recover seismic wave velocity of the surbsurface (Draganov et al., 2015). Focusing on surface waves, we produced a dispersion diagram from our cross-correlation signals. It reveals that the dominating signal is characterized by high frequencies between 30 and 90 Hz and has a velocity close to the acoustic wave velocity in water (Figure 13). Meanwhile, in the frequency band of surface wave exited by the airgun source (10-25Hz) our results only reveal faint signal that are not yet exploitable. At this stage these results are still preliminary and we will work at better characterizing this dominant signal by exploiting both vertical and horizontal sensors' records from all available GPR nodes and eventually look for other, less dominant signals

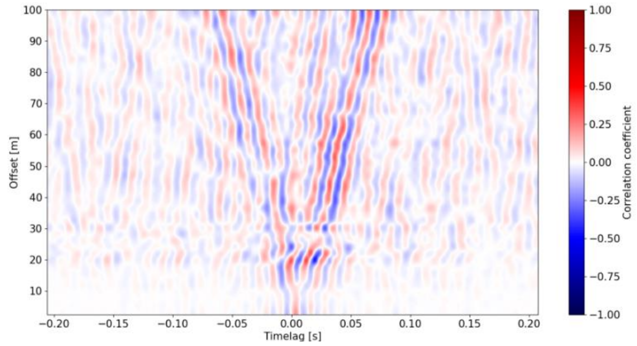

Figure 12 – Gather plot of the crosscorrelations calculated in the frequency range [10 ; 100] Hz for recordings of the vertical accelerometers on the center line with the CCN 301 during passive acquisition.

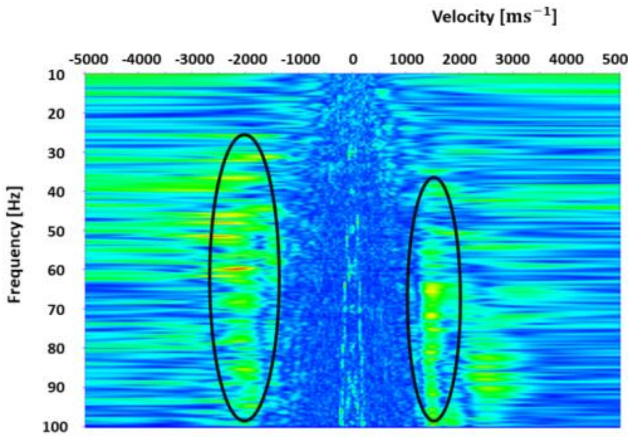

Figure 13 – Dispersion diagram calculated with the correlated data of figure 12.

5 CONCLUSIONS & PROSPECTIVES

The seismic measurement campaign carried out off Concarneau using 70 seabed sensors (GPR Sercel 4 components) tested the impact of the type of recording (accelerometer or hydrophone) and the position of the air-gun source on the recording of Sholte waves. Data analysis based on the calculation of dispersion diagrams shows that the seabed measurement system based on accelerometric sensors favors the recording of surface waves (Sholte waves) compared with hydrophone sensors.

The position of the air-gun source also influences the generation of Sholte waves. The latter are all the more pronounced in the recordings, particularly at lower frequencies, when the air-gun source is close to the seabed (5 m from the seabed in these tests). Based on these measurements, carried out at depths of almost 28 m in the near-shore, recordings of Sholte wave dispersion identifiable between 10 and 30 Hz correspond to wavelengths between 15 m and 85 m. This range of wavelengths is a priori favorable for the reconstruction of the Vs parameter linked to the small-strain shear modulus Gmax, for the first 30 m of the subsurface. In parallel with the tests carried out using air-gun sources, passive recordings made by leaving the sensors in place for 26 days show a coherent signal after cross-correlation of the recordings.

The corresponding dispersion diagrams show that the energy of the seismic signals is mainly related to acoustic propagation in the water column. Natural noise in the frequency range of interest, generally resulting from wave action on the coast or coastal human activity, is too low in the measurement zone. However, in principle, the passive approach does not require precise positioning of noise sources, and is therefore of great interest for marine measurements. An intermediate approach, using air-gun sources close to the seabed and located in areas at the ends of profiles or around all sensors but without precise positionning, would enable the energy carried by Sholte waves to be processed, based on cross-correlation of recordings. This approach, using so-called “opportunistic” sources, could be tested in future campaigns.

AUTHOR CONTRIBUTION STATEMENT

First and second authors: processing/analysis of active measurements. **Sercel authors:** sensor expertise. **Ifremer authors:** marine expertise, processing/analysis of passive measurements. **Second & all authors:** seabed measurements acquisition.

ACKNOWLEDGEMENTS

PROSE+ project is co-founded by Région Pays de Loire (RFI WEAMEC). Measurement are co-founded by Ifremer, Sercel, Gustave Eiffel Univ., OSUNA.

REFERENCES

Berthelot P., Puech A., Ropersf. (2019). Recommandations pour la conception et le dimensionnement des fondations d’éoliennes offshore. *Rapport du Groupe de Travail «Fondations d’éoliennes offshore» du Comité français de Mécaniques des Sols et de Géotechnique (CFMS)VERSION 2.0, 217 pp.* https://www.cfms-sols.org/sites/default/files/Rapport-cfms-eoliennes-offshore-2019-03-08-Version%20finale-BAT-HD.pdf

Draganov, D., Ruigrok, E. (2015). Passive Seismic Interferometry for Subsurface Imaging. In: Beer, M., Kougioumtzoglou, I., Patelli, E., Au, IK. (eds) Encyclopedia of Earthquake Engineering. Springer, Berlin, Heidelberg. https://doi.org/10.1007/978-3-642-36197-5_378-1.

Klein, G., Bohlen, T., Theilen, F., Kugler, S., & Forbriger, T. (2005). Acquisition and inversion of dispersive seismic waves in shallow marine environments. *Marine Geophysical Researches*, *26*, 287-315. DOI https://doi.org/10.1007/s11001-005-3725-6

Pageot, D., Leparoux, D., Capdeville, Y., & Côte, P. (2018, September). Alternative Surface Wave Analysis Method for 2D Near-Surface maging Using Particle Swarm Optimization. In *3rd Applied Shallow Marine Geophysics Conference* (Vol. 2018, No. 1, pp. 1-5). European Association of Geoscientists & Engineers. DOI: https://doi.org/10.3997/2214-4609.201802679

Park, C. B., Miller, R. D., & Xia, J. (1998). Imaging dispersion curves of surface waves on multi-channel record. In *SEG technical program expanded abstracts 1998* (pp. 1377-1380). Society of Exploration Geophysicists. DOI https://doi.org/10.1190/1.1820161

Strobbia, C., Godio, A., & De Bacco, G. (2006). Inversion of interfacial waves for the geotechnical characterisation of marine sediments in shallow water. *Bollettino Di Geofisica Teorica Ed Applicata*, *47*(1-2), 145-162.

Vanneste, M., Madshus, C., Socco, V. L., Maraschini, M., Sparrevik, P. M., Westerdahl, H., ... & Bjørnarå, T. I. (2011). On the use of the Norwegian Geotechnical Institute's prototype seabed-coupled shear wave vibrator for shallow soil characterization–I. Acquisition and processing of multimodal surface waves. *Geophysical Journal International*, *185*(1), 221-236. DOI https://doi.org/10.1111/j.1365-246X.2011.04960.x.

Wang, A., Rejiba, F., Bodet, L., Finco, C., & Fauchard, C. (2024). High-resolution surface-wave-constrained mapping of sparse dynamic cone penetrometer tests. *Near Surface Geophysics*, *22*(6), 666-680. DOI: https://doi.org/10.1002/nsg.12321